

Voltammetric Studies of Polymer Matrix Immunosensor Electrodes

Charlene D. Crawley and Garry A. Rechnitz*

Department of Chemistry and Biochemistry, University of Delaware, Newark, Delaware 19716

Received June 28, 1988

Galvanostatic and ac impedance experiments were carried out on potentiometric antibody sensors containing antigenic ionophores or antigen-ionophore conjugates in polymer membrane matrices. The changes in the charge-transfer resistance measured for varying concentrations of analyte are used as a diagnostic of the membrane response. It was determined that the potentiometric responses observed at these electrodes are due to a modulation of exchange currents by immunoreactions. In cases where the antigen can function as an ionophore for marker ion, conjugation to a separate carrier is not necessary and electrode construction is greatly simplified.

Introduction

Electrochemical biosensors have found wide usage in the analysis of body fluid metabolites and are more recently being developed for the detection of immunochemical substances as well.¹ Electrochemical immunoassays have been developed by using both amperometric² and potentiometric methodology.¹ Regardless of the technique used, however, the most critical sensor requirement is the ability to couple the high sensitivity and selectivity of immunochemical reactions with a suitable electrochemical transducer to obtain an analytically useful response. A possible means of achieving this goal involves the incorporation of antigen-ionophore conjugates in polymer membranes to produce potentiometric antibody-sensing electrodes. The analytical properties of such immunoelectrodes have already been described,³⁻⁶ but their mode of action has not been fully elucidated. It is the purpose of this paper to examine the electrochemical properties of such immunoelectrodes using galvanostatic and ac impedance techniques.

Neutral carrier ionophores, chosen for their lipophilicity and ability to form stable cation complexes within a polymer membrane, have been traditionally used in the construction of ion-selective electrodes for various alkali-metal ions. Such ionophores can be transformed into an immunoresponsive agent by chemical conjugation to an antigen or hapten. When such conjugates are immobilized in a polymer membrane, the resulting electrode shows a selective response to the appropriate antibody. In practice, the membrane is conditioned in and exposed to a constant activity of a marker ion, i.e., that ion that is specifically complexed by the ionophore portion of the conjugate, to attain a constant background potential. Upon addition of antibody capable of interacting with the antigen portion of the conjugate, the background potential is modulated in a manner that is proportional to the concentration of antibody (Ab). The technique that utilizes this kind of electrode system for the analysis of Ab concentrations is known as potentiometric ionophore modulation immunoassay (PIMIA) and has been described in detail for the analysis of antibodies to cortisol,³ dinitrophenol,⁴ digoxin,⁵ and quinidine.⁶

A typical prototype for such electrodes uses the hapten dinitrophenol (DNP) conjugated to a K⁺ ion neutral crown carrier, dibenzo-18-crown-6 (DBC), to form antigen-carrier

complexes. These complexes are dissolved in poly(vinyl chloride) (PVC) by using dibutyl sebacate as plasticizer in forming the polymer membrane. The membrane is placed in a hollow plastic housing between two reference electrodes. One side of the membrane is contacted by reference solution containing a constant concentration of K⁺ as the marker ion and the other side contacts an analyte solution containing antibody and marker ion in a high ionic strength buffer. The overall potentiometric response observed when antibody is added to the background analyte solution involves a change in the potential response of the neutral-carrier portion of the ionophore to marker ion associated with the selective binding of Ab to the DNP derivatized portion of the carrier (ionophore). It has been postulated that the interaction of the specific Ab to the antigen will in some way alter the interaction of the marker ion with the membrane phase. This perturbation in K⁺ ion transport would then alter the effective ion activity sensed by the membrane, resulting in a potential change related to the concentration of the specific antibody interacting with the membrane-bound hapten.

To test the validity of such hypotheses, voltammetric methods sensitive to the ion-transport properties of membranes have been used to ascertain a more complete picture of the Ab membrane interactions. The interfacial behavior of PVC membranes containing varying selectivity K⁺ ion neutral carriers was initially studied by using exchange current measurements⁷ as a first step toward understanding the nature of the Ab responses observed at these electrodes. In this paper we shall present results obtained for the more complicated derivatized carrier conjugates and their responses to both marker ion and antibody. The exchange current density is used to quantitate the selectivity of the derivatized carriers in the membrane to various analytes. Additional mechanistic information is obtained from ac impedance methods. These measurements may allow the separation of processes occurring at the interface of membranes from the processes occurring within the bulk of the membrane. It will be seen that surface immunoreactions modulate membrane exchange currents in systems where a potentiometric antibody response is observed.

Experimental Section

Apparatus. Potentiometric measurements were made with a Corning Model 12 pH meter and recorded on a Model SR-204 Heath/Zenith stripchart recorder. All experiments were conducted in a glass-jacketed cell thermostated at 30 °C with a Haake Model FS circulating temperature bath. The ac impedance and exchange current measurements were made with an EG & G

(1) Arnold, M. A.; Solsky, R. L. *Anal. Chem.* 1986, 58, 84R.

(2) Heineman, W. R.; Halsall, H. B. *Anal. Chem.* 1985, 57, 1321A.

(3) Keating, M. Y.; Rechnitz, G. A. *Analyst (London)* 1983, 108, 766.

(4) Solsky, R. L.; Rechnitz, G. A. *Anal. Chim. Acta* 1981, 123, 135.

(5) Keating, M. Y.; Rechnitz, G. A. *Anal. Chem.* 1984, 56, 801.

(6) Bush, D. L.; Rechnitz, G. A. *Z. Anal. Chem.* 1986, 323, 491.

(7) Crawley, C. D.; Rechnitz, G. A. *J. Membr. Sci.* 1985, 24, 201.

Princeton Applied Research (PAR) Model 362 scanning potentiostat/galvanostat with a Wavetek Model 187 pulse/function generator supplying the high-frequency sinusoidal waveforms. Transient responses greater than 1 Hz were recorded on a Houston Omnigraphic Model 2000 X-Y recorder. Potentials were monitored with a Keithley 169 digital multimeter. In-phase and out-of-phase ac components were detected with a PAR Model 5101 lock-in amplifier. A more detailed description of the experimental setup and cell design has been reported.⁷ All potentials are reported with respect to the Ag/AgCl (4.0 M KCl, saturated Ag) electrode with an Orion No. 90-01 sleeve-type single-junction reference electrode. PVC membranes were housed in a Model IS-561 Phillips electrode body that contained a AgCl anodized internal reference element.

Reagents. All standard chemicals were of analytical reagent grade, and all buffer and electrolyte solutions were made in distilled-deionized water. High-purity trizma base (Sigma) was used as the external supporting electrolyte. Dibutyl sebacate (Eastman) was also used as plasticizer for all membranes used. Chromatographic grade PVC was purchased from Polyscience Inc. Dinitrophenol, digoxin, and quinidine were purchased from Sigma and were used as received. Digoxin- and dinitrophenol (DNP)-dibenzo-18-crown-6 conjugates were synthesized in our laboratories by using previously reported procedures.⁵

Antibodies to DNP (61006, Lot R910, titer 1.2 mg of Ab/mL) and digoxin (65-855, Lot 5553, titer 0.22 mg of Ab/mL, and Lot 5554, 0.16 mg of Ab/mL) were purchased from Miles Laboratories as the rabbit bovine-serum albumin (BSA) antisera. Antibody concentrations were estimated from Scatchard's equation with information available from the manufacturer. BSA antibodies were purchased from Miles in lyophilized form (titer 2.6 mg of Ab/mL). All antibody solutions were extensively dialyzed in background buffer/electrolyte solutions with Spectrophor dialysis tubing (MW cutoff 3500). Background solutions contained 0.1 M Tris/HCl (pH 7.4), 0.034 M $\text{CaCl}_2 \cdot \text{H}_2\text{O}$, and 0.001 M KCl.

Procedures. Membrane Preparation. The membranes were prepared by dissolving 250 mg of PVC, 300 μL of dibutyl sebacate ($\rho = 0.936$) and varying milligram quantities of carrier in tetrahydrofuran. Resultant membranes were cast in 9.5-cm-diameter petri dishes and were allowed to cure a minimum of 24 h before use. Membrane concentrations are expressed either as total milligram quantities of carrier per batch or as the fraction of carrier present per each individual electrode, micrograms/disk. The thickness of the membranes varied between 0.03 and 0.09 mm. Membrane disks assembled in the electrode had an area of 0.28 cm^2 ; however, the electrode contact area was 0.12 cm^2 . Internal reference solutions contained 0.01 M KCl, and the outer membranes were conditioned either in 0.1 M KCl or in pH 7.5 Tris/HCl buffer solutions.

Voltammetric Techniques. Exchange current measurements were obtained from analysis of the transient response to current perturbation of the membrane. A nanoampere current pulse was applied through the internal reference element of the electrode, and the resultant potential difference monitored as a function of time. The current step pulses were applied successively in solutions containing varying concentrations of analyte. Detailed procedures used in obtaining exchange current data using the galvanostatic step method have been reported.⁸

The current-overpotential diagrams were obtained by potentiostatic control of the potentials at the membrane while the current was measured as a function of time. Potentials ranging from 20 mV to 2 V were applied to the Ag/AgCl element of the internal reference electrode. The overpotential, η , is equal to the difference in the applied potential and the equilibrium potential values.

The ac impedance data were obtained by applying a 250 mV root-mean-square (2.5×10^{-7} A) amplitude sinusoidal current signal through the internal reference element of the electrode at varying frequencies (5–50 kHz) and measuring in-phase and out-of-phase components of the resultant potential responses. Cole-Cole plots of the real and imaginary impedances were used to calculate the RC network elements used to model the membrane interface.

	CARRIER	ANTIGEN - DBC CARRIER COMPLEX	ANTIGEN	BLANK MEMBRANE
Membrane Components	Valinomycin Dibenzo-18 crown-6 (DBC) PVC - alone	DNP - DBC Digoxin - DBC	Digoxin DNP	Plasticizer
Analyte	K^+	K^+ Anti - DNP Anti - Digoxin Anti - BSA	K^+ Anti - DNP Anti - Digoxin	K^+ Anti - DNP Anti - Digoxin Anti - BSA

Figure 1. Summary of experimental studies employed.

Results and Discussion

Diagnostic Descriptors of Membrane Response.

Pertinent questions to be addressed in diagnostic studies of the antibody electrode are the following:

1. How is the membrane selectivity to antibody and marker ion affected by chemical modification of the neutral carrier?
2. Is the potentiometric response attributed to and primarily selective for the specific antibody?
3. What is the nature of the "perturbation" of the carrier in the membrane that gives rise to an antibody potential signal?

A summary of the experimental logic employed in addressing the above listed questions is shown in Figure 1. The first phase focused on studying the response of neutral carriers having varying selectivities for the marker ion, K^+ , in a polymer matrix of poly(vinyl chloride). We then studied two cases in which the comparatively low-selectivity carrier dibenzo-18-crown-6 (DBC) was derivatized by conjugation with digoxin or DNP antigens. The responses of the antigen-carrier conjugates were observed to marker ion in the presence and absence of the respective antibodies and also to anti-BSA (a nonspecific antibody). The responses of the unconjugated antigens alone are presented for the same analytes. Finally, the blank case is that in which the membrane component is just plasticizer.

The first question regarding selectivity of the derivatized and underivatized carriers will be addressed from the standpoint of the apparent exchange current densities. The potentiometric selectivity of the carriers in the membrane is directly related to the magnitude of the exchange current obtained for analyte. This exchange current, as applied to ion-selective electrodes (ISEs), can be described as the net current produced by the movement of ions into and out of the membrane interface at equilibrium. If the exchange current density is large for a particular ion, then the electrode, membrane, etc., involved is primarily selective for that ion. This is shown in Figure 2 for polymer membranes containing the underivatized K^+ ion carriers. The current-overpotential diagrams shown were obtained by using the potential step method in which the potential across the membrane was controlled and the current was measured as a function of time. The analyte in all three cases is marker ion solution, 0.029 M KCl. It can be seen that much larger currents are obtained at lower overpotentials for membranes containing the high-selectivity carrier valinomycin as compared to the negligible currents obtained for the blank membrane at significantly larger overpotentials. The current-overpotential curves obtained from potential step measurements will be utilized in this study only as a means of qualitatively visualizing the im-

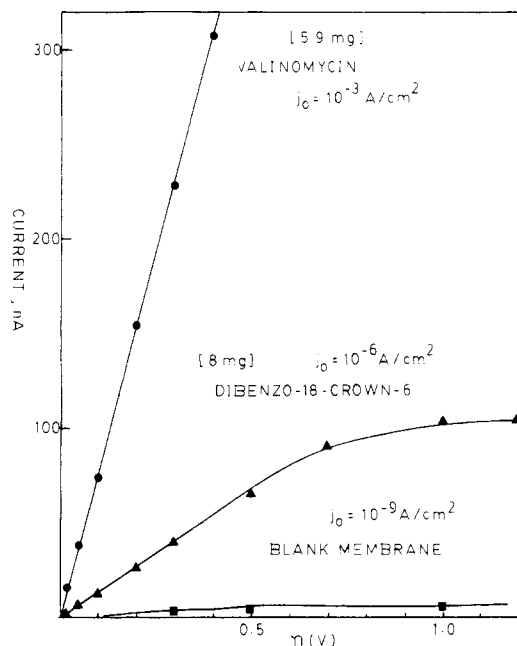


Figure 2. Current-voltage curves for membranes containing varying selectivity K^+ ion neutral carriers.

pect of chemical derivatization of the carrier on its response to marker ion.

The membrane thickness is comparable in each of the three cases shown so that the dominant effect observed is due to the differing K^+ exchange currents of each of the carriers within the membrane. However, the bulk membrane resistances are often difficult to reproduce from membrane to membrane; therefore, the current step method was used to estimate the exchange current density since, in certain cases, corrections for the background resistances could be applied. Nevertheless, these values can be considered only as apparent values, due to both the assumptions utilized in the technique and the ever-present background resistances attributable to the bulk of the membrane.

The second question that addresses the identity of the potential determining species, e.g., that species which predominantly contributes to the observed potential changes, is also probed with current step experiments. With the galvanostatic-step method, the charge-transfer resistance could be calculated for each case. Generally this parameter, which is also related to the activation energy for charge transport, is dependent on the concentration of analyte. Results from these studies on polymer membranes containing varying selectivity neutral carriers have shown that the concentration dependence of the charge-transfer resistance, R_{CT} could also be utilized as a diagnostic for discerning the identity of the potential determining species.

The R_{CT} behavior is diagrammatically shown in Figure 3 for the underivatized carriers where cases I–III are representative of the overpotential–time responses for the blank membrane, membranes containing DBC, and valinomycin, respectively, to increasing concentrations of marker ion. For the high-selectivity carrier, valinomycin, shown as case III, the morphology of the overpotential response shows very little impact from membrane diffusional polarization. Furthermore, the overpotentials decrease as the K^+ analyte concentration increases. A plot of $\log R_{CT}$ versus $\log [\text{analyte}]$ is linear and has a negative slope. This slope remained negative for membranes having concentrations in the range 1–24 $\mu\text{g}/\text{disk}$. The opposite

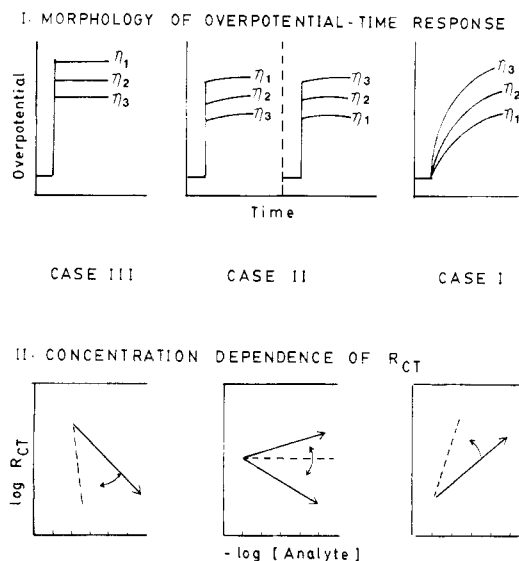


Figure 3. Summary of results obtained from exchange current measurements on membranes containing valinomycin (case III); dibenzo-18-crown-6 (case II), and just plasticizer alone (case I). The overpotential, η , response is shown for increasing additions of K^+ marker ion as indicated by the numbered subscripts.

trend is apparent in case I, the nonselective blank PVC membrane. The overpotentials increase as the $[K^+]$ analyte increases, there is a much larger impact from membrane diffusional polarization, and longer times are required to reach a steady-state potential. The resultant R_{CT} plots are linear with a positive slope.

Finally, the low-selectivity DBC carrier shown as case II exhibits behavior similar to that observed in cases I and III depending on the concentration of crown within the membrane. For the high concentrations of crown studied ($>15 \mu\text{g}/\text{disk}$) responses characteristic of valinomycin are observed, i.e., linear R_{CT} plots, having a negative slope. When the concentration of carrier was less than 10–0.1 $\mu\text{g}/\text{disk}$, responses similar to the blank membrane case were observed, however with much less diffusion effects exhibited in the η vs time transients.

From these results we have concluded that the responses obtained for the high-selectivity case III, i.e., linear $\log R_{CT}$ vs $\log [\text{analyte}]$ plots with a negative slope, are an indicator that the species being monitored is the "potential-determining species". Likewise, responses modeling case I behavior, i.e., positive slope in the $\log R_{CT}$ vs $[\text{analyte}]$ plot, are not indicators of specificity. The criteria developed from cases I–III can now be utilized as a guideline for isolating the potential determinant and discerning whether the potentiometric responses observed at these membranes are attributed to and selective for the corresponding antibodies. In the following discussions, both the current-overpotential diagrams and the charge-transfer resistance behavior will be described for both marker ion and antibody at membranes containing various carriers.

Antigen-Carrier Conjugates. DNP-DBC Conjugates. Membranes having comparable concentrations of DBC and DNP-DBC conjugate both gave a significant response to K^+ marker ion. However, the slopes of the potentiometric concentration calibration curves decreased slightly, from 56.4 to 52.9 mV/decade at 30 $^{\circ}\text{C}$, with about a 1-decade decrease in sensitivity, from 10^{-4} to 10^{-3} M KCl, in going from the DBC to the DNP-DBC conjugate.

A more dramatic difference is seen in the current-overpotential diagrams of the two cases as shown in Figure 4. Though the membrane thicknesses are comparable, i.e., 0.06 and 0.04 mm for DBC and DNP-DBC conjugate,

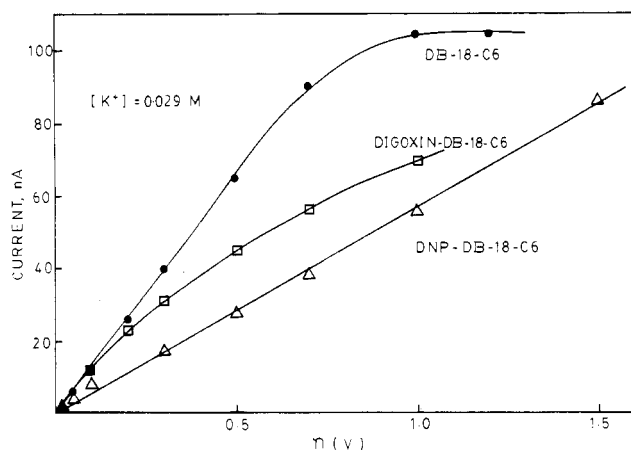


Figure 4. Current-voltage curves for membranes containing the crown and derivatized crown carriers: ●, 8 mg of dibenzo-18-crown-6; □, 7.96 mg of digoxin-dibenzo-18-crown-6 conjugate; △, 7.3 mg of dinitrophenol-dibenzo-18-crown-6 conjugate.

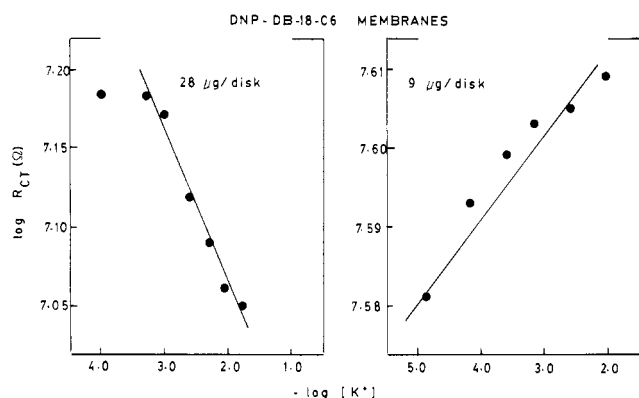


Figure 5. Comparison of charge-transfer resistance responses for membranes containing 28 and 9 $\mu\text{g/disk}$ concentrations of the dibenzo-18-crown-6 (DBC) conjugate.

respectively, the magnitude of current flowing across the interface in the presence of 0.029 M KCl is clearly larger for the DBC. This deviation could be due to the derivatization of the crown, which might result in a less stable K^+ -crown complex, though the complex still retains the ability to function as a carrier for marker ion.

The potentiometric response of the antigen conjugate membranes to antibody increases upon reduction of the concentration of the DNP-DBC conjugates within the membrane;⁶ however, this also results in a concurrent loss in response to marker ion. This effect is exemplified in the exchange current data for decreasing concentrations of the DNP-DBC conjugate within the membrane. At the high concentration of carrier shown in Figure 5, e.g., 28 $\mu\text{g/disk}$, the charge-transfer resistance is linear and has a negative slope for increasing concentrations of marker ion in solution, which is indicative of a selective response. As the membrane concentration of conjugate is lowered to 9 $\mu\text{g/disk}$, the overall membrane resistances increase and the slope of the $\log R_{CT}$ vs $\log [\text{K}^+]$ plot becomes positive, which is indicative of a loss in selectivity. This slope becomes increasingly more positive for membranes containing 1.0 and 0.1 $\mu\text{g/disk}$ DNP-DBC conjugate.

Optimal antibody response was observed for membranes containing the lower concentration of conjugate, i.e., 0.1 $\mu\text{g/disk}$. Diffusion-corrected overpotential-time responses obtained by using the current step method for varying concentrations of anti-DNP are shown in Figure 6 at a membrane containing 0.1 $\mu\text{g/disk}$ DNP-DBC conjugate. In the range 10–50 μg antibody/mL, the overpotentials

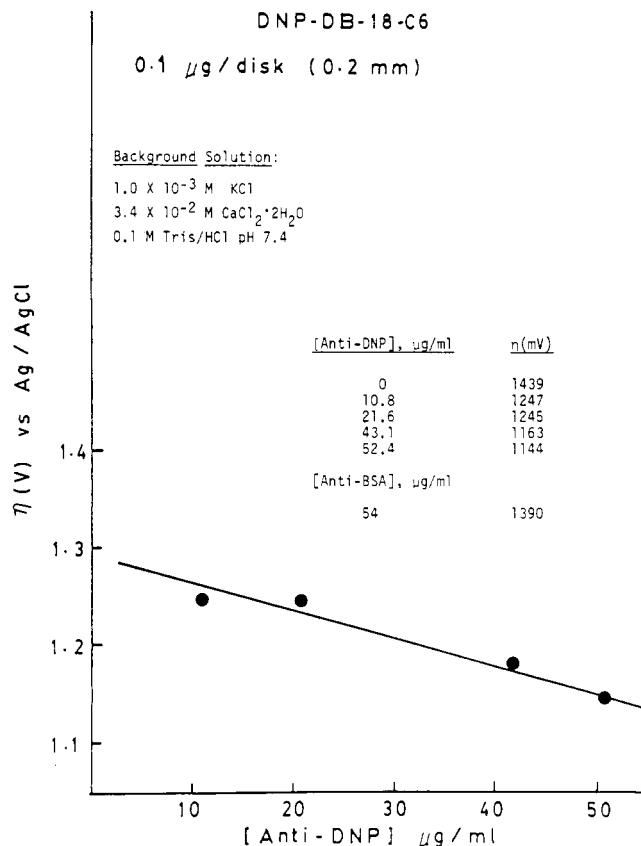


Figure 6. Overpotential responses generated upon application of nanoamp currents through a 0.2-mm-thick membrane containing 0.1 $\mu\text{g/disk}$ DNP-dibenzo-18-crown-6 conjugate for varying concentrations of DNP antibody.

become smaller as the concentration is increased. Upon addition of a comparable amount of anti-BSA the overpotential increases. This shows then that the responses observed are not due to nonspecific protein adsorption processes occurring at the membrane interface. The overpotential, η , is directly proportional to R_{CT} ; therefore, this plot is equivalent to a R_{CT} vs [anti-DNP] analyte plot having a negative slope and is thus indicative of a selective response.

Due to the quite large overpotentials observed at a 0.2-mm-thick membrane, i.e., potentials in excess of 1 V, these experiments were repeated on thinner membranes, having thicknesses in the range 0.06–0.08 mm. The same trend was observed; however, the slopes were even more negative due mainly to the less pronounced impact of the smaller bulk membrane resistance in the overall charge-transfer resistance responses. Even more interesting is the fact that the range of antibody concentrations that gave a linear response in the R_{CT} plot remains essentially the same for the thinner membranes, which is also approximately the same range of antibody concentrations giving an increasing potentiometric response to antibody. The R_{CT} response for anti-BSA gave a corresponding plot with a positive slope at membranes containing the same concentration of DNP-DBC conjugate, as shown in Figure 7. As a test of whether such a low concentration of DNP-DBC conjugate was actually the predominant carrier species in the antibody reaction, the same 10–50 $\mu\text{g/mL}$ concentration range of anti-DNP was added, and the exchange current measurements were repeated at a blank PVC membrane containing just plasticizer. The R_{CT} vs [anti-DNP] plot also had a positive slope (Figure 7), which shows that the presence of the carrier conjugate is needed

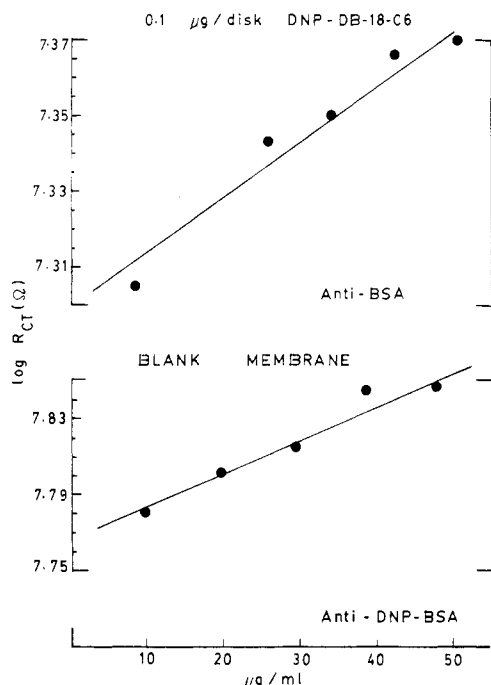


Figure 7. Comparison of the charge-transfer resistance behavior for two membranes. The top trace shows the response obtained for anti-BSA at a membrane containing 0.1 μg /disk DNP-dibenzo-18-crown-6 conjugate. The bottom trace shows the DNP antibody at a blank PVC membrane containing just plasticizer (dibutyl sebacate).

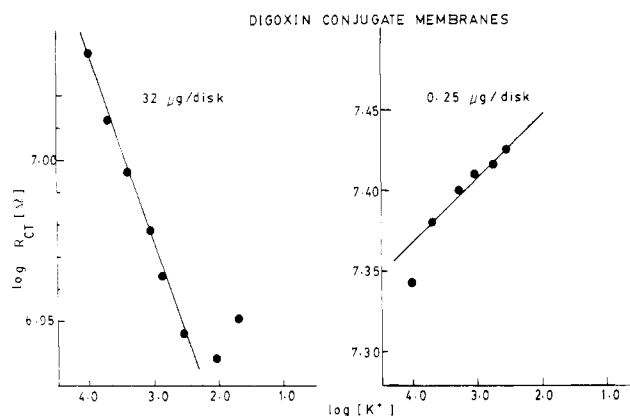


Figure 8. Comparison of charge-transfer resistance responses for membranes containing 32 and 0.25 μg /disk of digoxin-dibenzo-18-crown-6 conjugate.

and does govern the responses observed even at the low concentration levels.

Digoxin-DBC Conjugate. The same behavior exhibited by DNP is obtained when digoxin is conjugated to the crown carrier. The potentiometric response is essentially the same in that both the slopes of the calibration curve and the sensitivity to marker ion are comparable. However, when viewing the current-overpotential curves, there is a small diminution in marker ion current as compared with the DBC carrier alone, although not as low as that observed with the DNP-DBC conjugate. A comparison of the charge-transfer resistance responses obtained for membranes containing 32 μg /disk concentrations of digoxin-DBC conjugate versus a membrane containing 0.25 μg /disk is shown in Figure 8. The overall membrane resistance increases and the slope of the $\log R_{CT}$ vs \log [analyte] plot is positive for the lower concentration of carrier conjugate. From these results, we can conclude that the response to marker ion is governed by the ionophore

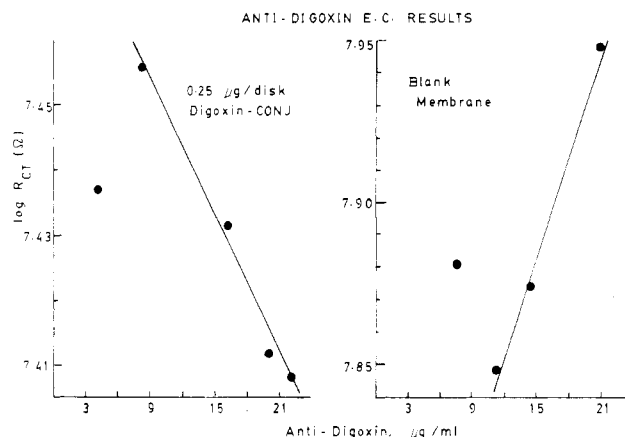


Figure 9. Comparison of the charge-transfer resistance responses obtained for anti-digoxin at a digoxin-dibenzo-18-crown-6 conjugate (left) containing membrane and at a blank membrane (right) containing just plasticizer.

portion in both cases involving the antigen-carrier complexes and each mimicks the response of the DBC carrier alone.

The R_{CT} responses obtained for anti-digoxin antibody at a membrane containing a low concentration of the digoxin-DBC conjugate, 0.25 μg /disk, and a blank membrane are compared in Figure 9. The same trends are seen as with the DNP-DBC cases, except that now the effective antibody concentration range is decreased to the 9–22 μg /mL range of anti-digoxin. This region of antibody concentrations also corresponds to the optimal potentiometric response ranges.

Antigens Alone. The exchange current measurements reported show that the chemically conjugated antigen carriers do not interfere to any great degree with the ability of the neutral crown carrier to complex K^+ marker ions. The next point of interest, then, is studying how the antigen alone influences the potentiometric responses to marker ion and antibody. This has been tested for the DNP and digoxin antigens alone, which were immobilized in PVC membranes with just plasticizer.

DNP Alone. Current-overpotential curves were constructed for a membrane containing a 1.0 μg /disk concentration of DNP in the presence of 0.029 M KCl marker ion solution. The results are compared with the response obtained for a high concentration of DBC in Figure 10. Dinitrophenol is capable of complexing K^+ ions and has an affinity constant of $\log K = 1.94$,⁹ which is similar to that exhibited by the crown ether, DBC. However, the larger currents obtained for K^+ would suggest that DNP can function as a very good carrier species even at much lower concentrations within the membrane than the DBC carrier alone. Membranes containing relatively high concentrations of DNP (8.1 mg of stock, 32 μg /disk) had membrane resistances in excess of $10^8 \Omega$, which were untenable to potentiostatic control; therefore a comparison of the concentrated DNP membrane with that containing a high concentration of DBC could not be attained.

The $\log R_{CT}$ vs $\log [K^+]$ plots were linear, with negative slopes for membranes containing 1.0 and 0.1 μg /disk concentrations of DNP, indicating that both low-level concentrations give a selective response to marker ion. The 0.1 μg /disk concentration of DNP also gave a selective antibody response in the same antibody concentration range as obtained for the 0.1 μg /disk DNP-DBC conjugate

(9) IUPAC, *Stability Constants of Metal-Ion Complexes Part B*; Pergamon Press: New York, 1979.

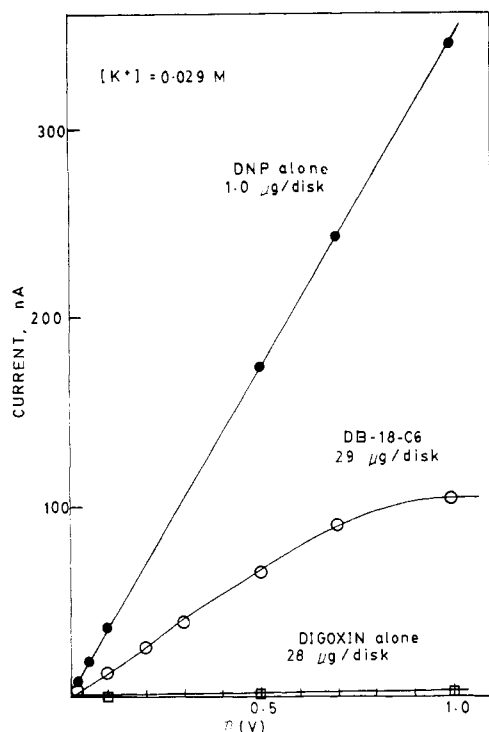


Figure 10. Current-voltage curves for membranes containing the antigens alone: ●, 1.0 $\mu\text{g}/\text{disk}$ dinitrophenol; ○, 29 $\mu\text{g}/\text{disk}$ dibenzo-18-crown-6; □, 28 $\mu\text{g}/\text{disk}$ digoxin alone.

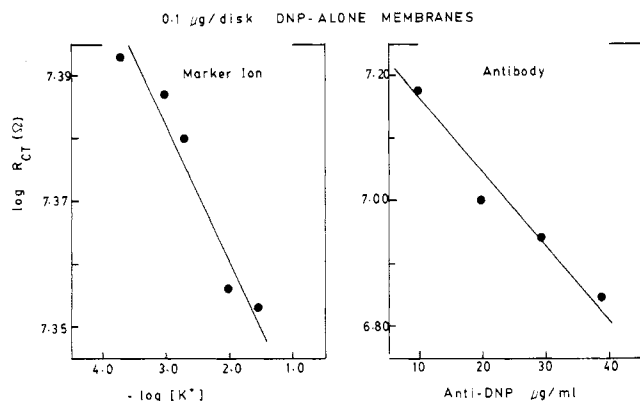


Figure 11. Comparison of the charge-transfer resistance responses obtained for K^+ marker ion and anti-DNP antibody at a membrane containing 0.1 $\mu\text{g}/\text{disk}$ dinitrophenol.

membranes, as shown in Figure 11. These results then show that chemical conjugation of the antigen to an ionophore is not needed if the antigen exhibits carrier properties for marker ion. Though only systems responding to K^+ marker ions are presented in this article, other marker ions can also be used. The anti-quinidine antibody electrode serves as an example of this wherein quinidine was immobilized in a PVC membrane and served as both an antigen and a carrier for protons.⁶

Digoxin Alone. Both the potentiometric concentration calibration plots and the current-overpotential diagrams for analyte solutions containing marker ion were essentially no different at membranes containing a high concentration of digoxin alone (28 $\mu\text{g}/\text{disk}$) from that observed at a blank PVC membrane (see Figure 10). Furthermore, there was essentially no change detected in the charge-transfer resistance behavior of these membranes upon addition of marker ion. This evidence, coupled with a knowledge of the chemical structure of digoxin, which is a steroid, demonstrates that digoxin alone does not behave as a K^+ ion carrier. In addition, R_{CT} plots for anti-digoxin an-

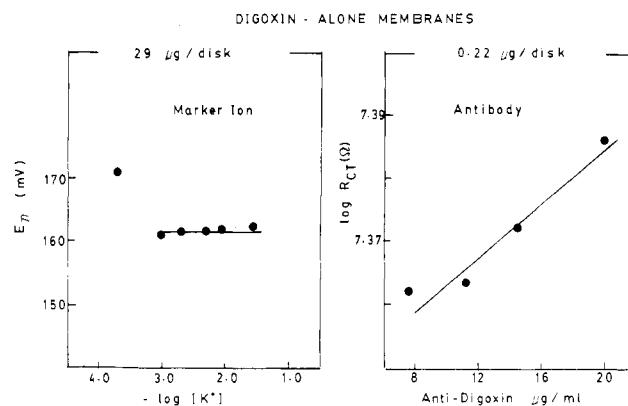


Figure 12. Results from applied current measurements at a membrane containing just digoxin. The left trace shows the overpotential changes obtained upon addition of K^+ marker ion at a membrane containing 29 $\mu\text{g}/\text{disk}$ digoxin. The right trace shows the charge-transfer resistance responses for increasing concentrations of digoxin antibody at a membrane containing 0.22 $\mu\text{g}/\text{disk}$ digoxin.

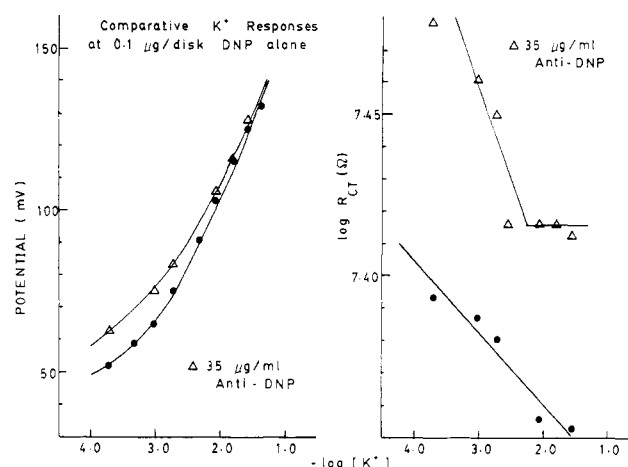


Figure 13. Comparison of marker ion responses with and without antibody present at a membrane containing 0.1 $\mu\text{g}/\text{disk}$ of dinitrophenol. The left trace shows the potentiometric responses for increasing concentrations of K^+ in just background electrolyte, ●, and after the addition of 35 $\mu\text{g}/\text{mL}$ of DNP antibody to the background electrolyte, △. The right trace shows the corresponding charge-transfer resistance responses under the same conditions.

tibody yield a positive slope for membranes containing a low concentration of digoxin, as shown in Figure 12, which is not indicative of a selective response to antibody. Therefore, in this case, digoxin must be conjugated to an extraneous ionophore to elicit an antibody response.

Comparative Effects of Antibody on Marker Ion Response. The membrane containing only DNP was chosen as the best test case to probe if the antibody does indeed cause a perturbation in the response of the carrier to marker ion. Exchange current results have shown that low levels of DNP in membranes will function both as a carrier for K^+ marker ion and as a selective hapten for antibody. Therefore any loss in the ability of DNP to respond to marker ion in the presence of antibody would be more clearly observed with this system.

The potentiometric response to marker ion is compared with the corresponding marker ion response in a solution having a 39 $\mu\text{g}/\text{mL}$ background of DNP antibody in addition to electrolyte in Figure 13, left. A more drastic comparison of the two cases is observed in the charge-transfer resistance data as shown in Figure 13, right. The bottom trace of Figure 13, right, (solid circles) shows that

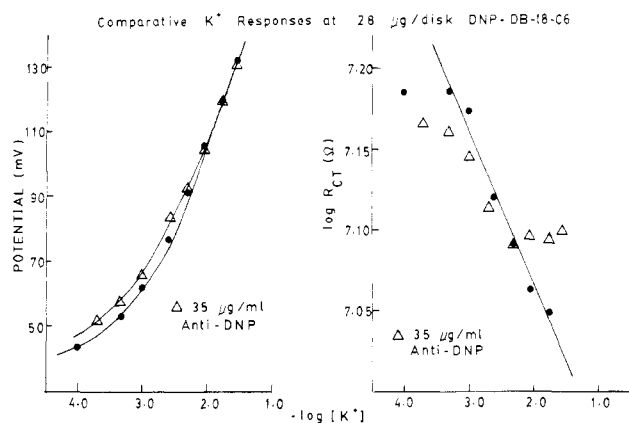


Figure 14. Effect of antibody on the response of a membrane containing 28 $\mu\text{g}/\text{disk}$ of the DNP-dibenzo-18-crown-6 conjugate to K^+ marker ion. The left trace shows the comparative potentiometric responses, \bullet , without antibody, and with 35 $\mu\text{g}/\text{mL}$ of DNP antibody, Δ .

the membrane did yield the expected selective marker ion response for increasing concentrations of K^+ in buffered background electrolyte. The top trace (open triangles) is also indicative of a selective marker ion response and was obtained upon addition of potassium to background electrolyte containing 39 μg of anti-DNP/mL. Note that the charge-transfer resistances are now shifted to higher values and begin to level off at high K^+ concentrations. Since the exchange current is inversely related to the charge-transfer resistance, the effect observed represents a decrease in the exchange current for marker ion due to the presence of the antibody.

Such a dramatic effect was not obtained when the same experiment was repeated at a membrane containing a high concentration of the DNP-DBC conjugate as depicted in Figure 14. Although there is some impediment in the ability of the carrier to respond to marker ion at high concentrations of K^+ (i.e., a leveling off in the R_{CT} response) due to the presence of antibody, the impact on the exchange current response is not as drastic. This is not surprising considering that the antibody response is lower at membranes containing a higher concentration of the antigen-crown conjugate. Therefore, one could also conclude that the larger antibody response obtained at the membranes having a lower concentration of immobilized carrier is a result of a much higher fraction of that carrier being controlled by the antigen-antibody interactions.

Results from the exchange current measurements can be summarized pictorially in Figure 15, which shows a schematic representation of the polymer membrane sandwiched between the reference and analyte solutions. The arrows within the membrane represents the pool of carrier complex that is available for complexation with marker ion. Upon complexation, the movement of ions within the membrane and/or across the interface will generate a corresponding current. The magnitude of this current flux is related to the exchange current density. Upon addition of Ab to the analyte solution, the pool of carrier available for uptake of marker ion is decreased due to immobilization of carrier by the surface immunoreaction. The increase in the R_{CT} response for marker ion measured in the presence of antibody at the 0.1 $\mu\text{g}/\text{disk}$ DNP-alone membrane reflects this perturbation in the response of carrier to marker ion. Therefore, the exchange current density of the carrier to K^+ marker ion is most likely the parameter that is being modulated to produce potential changes proportional to the concentration of added antibody.

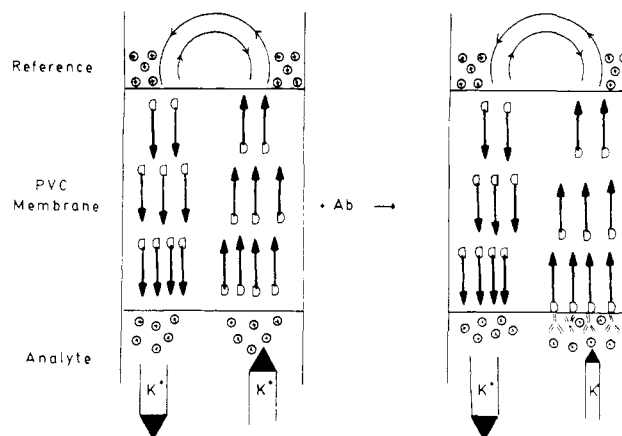


Figure 15. Model depicting the role of exchange currents at the potentiometric antibody electrode.

AC IMPEDANCE METHOD

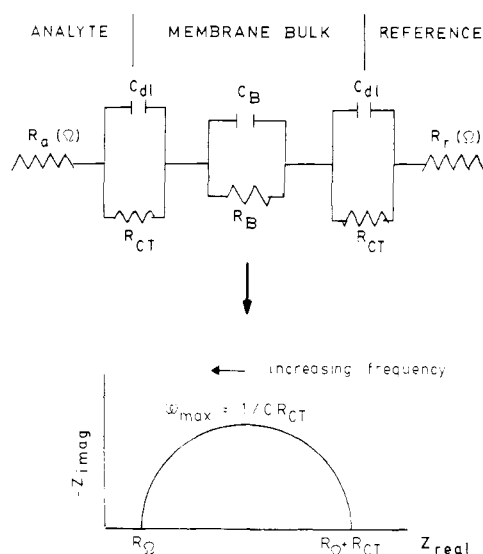


Figure 16. Diagram of the membrane equivalent circuit elements analyzed in the ac impedance experiment: R_a , R_r = analyte and reference solution resistances; R_{CT} = charge-transfer resistance; C_{dl} = double-layer capacitance; R_B = bulk membrane resistance; C_B = bulk membrane capacitance.

Ac Impedance Results. Additional information concerning the processes occurring at these electrodes can be obtained from ac impedance measurements.¹⁰ Interfacial processes occurring at ISEs can be described in terms of equivalent electrical circuits consisting of parallel resistance capacitance networks as shown in Figure 16. The capacitance, C_{dl} , models the behavior of the charged interfacial layer and can also be related to the identity and magnitude of charge carriers present. The resistive component, R_{CT} , represents the resistance to charge transfer across the interface and is related to the exchange current density. R_B and C_B are the corresponding components as applied to the interior of the membrane.

Typically, three regions can be recognized from the analysis of the ac impedance behavior of ion-selective electrodes.¹¹ These three regions are separated in terms of the time constants of the processes occurring within their domain and can be experimentally isolated by ad-

(10) Buck, R. P. In *Ion Selective Electrodes*; Pungor, E., Ed.; Elsevier: New York, 1981; Vol 3.

(11) Moody, G. J. *J. Biomed. Eng.* 1985, 7, 183.

Table I. Comparison of Ac Impedance Marker Ion Response

membr ^a component	analyte ^b	R_{CT} , Ω	C_{dl} , F	τ_{dl} , ms	R_B , Ω	C_B , F	τ_B , ms
DNA alone	0.1	2.0×10^6	3.2×10^{-9}	6.4	5.5×10^6	7.2×10^{-11}	0.4
	0.001	5.0×10^5	2.1×10^{-8}	10.6	1.6×10^6	1.0×10^{-10}	0.2
DNP-DBC ^c	0.1				9.6×10^6	6.6×10^{-11}	0.6
	0.001				1.6×10^7	6.6×10^{-10}	1.1

^a0.1 $\mu\text{g}/\text{disk}$. ^bMolar KCl marker ion concentration. ^cDNP-DBC; dinitrophenol-dibenzo-18-crown-6 conjugate.

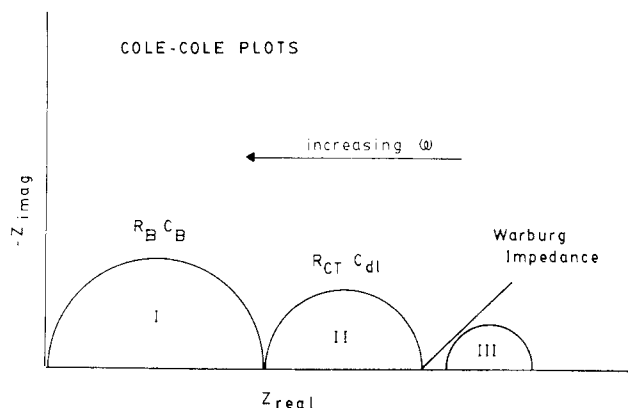


Figure 17. Diagram of the distinct RC network zones analyzed from Cole-Cole plots.

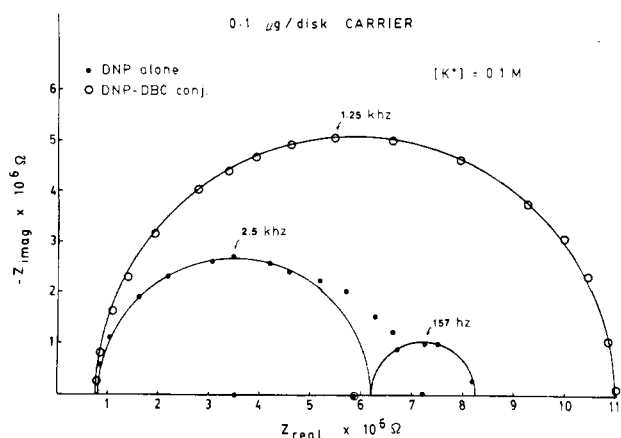


Figure 18. Comparison of the Cole-Cole plots obtained for K^+ marker ion response at membranes containing $0.1 \mu\text{g}/\text{disk}$ of DNP, \bullet , and DNP-dibenzo-18-crown-6 conjugate, \circ . The frequencies, f , shown are the radial frequencies, where $\omega = 2\pi f$.

justing the frequency of the applied ac perturbation. A popular means of evaluating ac impedance data is through the use of Cole-Cole or Nyquist plots, which produce semicircles that are indicative of RC type behavior at varying frequencies. The x axis, Z_{real} , of this plot is the ac equivalent of the resistance that is measured 0° in phase with the applied perturbation. The y axis, Z_{imag} , is the so called "imaginary" impedance element that is measured 90° out-of-phase with the applied reference signal. The magnitude of the resistive component is determined from the diameter of the semicircle. As shown in Figure 17, the movement of charged carriers within the bulk of the membrane is observed at higher frequencies than the slower interfacial and/or surface processes occurring at the membrane. Warburg diffusion of charge carriers covers the lower frequency ranges extending from about 10 to 0.001 Hz. A portion of the Warburg impedance semicircle forms a line that has a 45° angle with the real axis, is indicative of mass-transfer-limited processes, and is also diagnostic of charge carriers that actually pass through the interface.

Cole-Cole impedance plots for membranes containing $0.1 \mu\text{g}/\text{disk}$ concentrations of DNP alone are compared

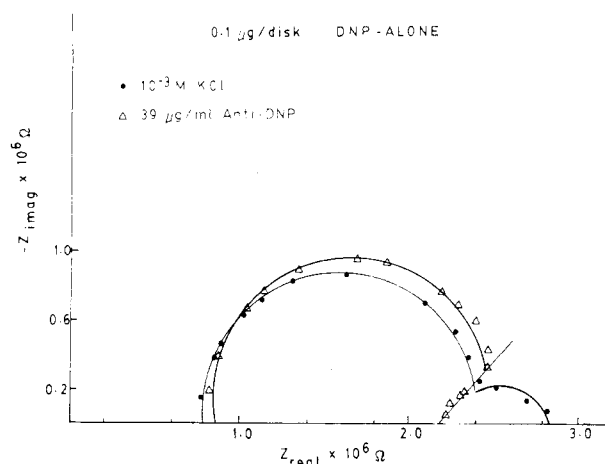


Figure 19. Cole-Cole plots for DNP alone membranes in response to K^+ marker ion in background/electrolyte solution, \bullet , and with the addition of DNP antibody, Δ .

with those obtained for a membrane containing a comparable concentration of the DNP-DBC conjugate as shown in Figure 18 for 0.1 M KCl analyte solutions. Individual impedance elements are also tabulated in Table I. Only one semicircle was obtained for the latter crown conjugate case within the frequency region covered (5–50 kHz). However, these data show that the bulk resistances are lower for the DNP-alone membrane as compared with the DNP-DBC conjugate case and the interfacial charge-transfer resistances are even lower for the former membrane. These results concur with the applied current data in that conjugation of the DNP group to the crown does appear to interfere with the ability of both carriers to function as ionophores for marker ion, therefore resulting in an increase in the resistance of the membrane.

One of the major advantages of the ac impedance method is that one can obtain a qualitative picture of the reactions occurring at the membranes in addition to the ability to simultaneously separate and quantitate parameters indicative of the separate processes observed. Second, the ac impedance technique is a steady-state method that does not significantly disturb the equilibrium of the membrane. Figure 19 gives the comparative Cole-Cole plots obtained for a $0.1 \mu\text{g}/\text{disk}$ DNP alone to two analyte species. The solid circles represent the response obtained for a 10^{-3} M KCl marker analyte in background buffer/electrolyte solution, and the triangles represent the analogous plot obtained for the same membrane but with the addition of $39 \mu\text{g}/\text{mL}$ of anti-DNP antibody solution. Two features are worth noting. First, the interfacial regions for the two analytes are distinct. While the expected semicircle is obtained for K^+ marker ion alone, when the antibody is added, a response more diagnostic of a Warburg impedance is obtained, i.e., a linear region forming a nearly 45° angle with the x axis of the Cole-Cole plot. This behavior is indicative of a mass-transfer-limiting process occurring across the membrane interface and could be attributed to the antigen-antibody surface immunoreaction. Furthermore, the capacitance element, C_B , which

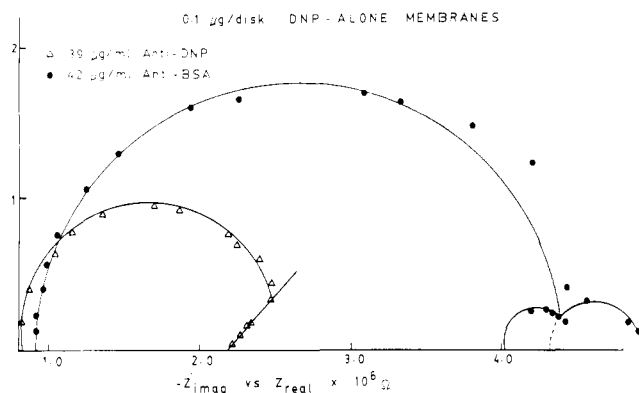


Figure 20. Comparison of impedance responses to anti-DNP, Δ , and to anti-BSA, \circ , at a membrane containing 0.1 $\mu\text{g/disk}$ DNP alone.

represents the magnitude of charge carriers within the interior of the membrane, is essentially the same when exposed to marker ion and antibody. This would not be expected if the binding of antibody to antigen was significantly removing DNP (antigen carrier) from within the interior of the membrane.

This notion is also supported in a second experiment where a membrane containing a 1.0 $\mu\text{g/disk}$ concentration of DNP alone was exposed to analyte solution containing 109 μg of anti-DNP/mL for 2.5 h with stirring. The ac impedance plot was obtained before and after conditioning

in antibody and, in each case, the solutions contained 10^{-3} M KCl in buffer/electrolyte. Though the membrane bulk resistance component increased from 10.4 to 13.2 M Ω , the bulk capacitive component still remained essentially the same, i.e., from 1.02×10^{-10} to 1.0×10^{-10} F.

Finally, the ac impedance plot for a 0.1 $\mu\text{g/disk}$ DNP-alone membrane exposed to comparable concentrations of anti-DNP and anti-BSA are shown in Figure 20. Clearly the overlapping semicircles obtained at low frequencies for the anti-BSA analyte are different than the behavior observed for the selective DNP antibody. This indicates that the interfacial features cognizant in a selective protein adsorption process are characteristically distinct from the nonselective adsorption-type interaction depicted for anti-BSA. This would be expected on the basis of an additional binding affinity for the interaction of a specific antibody with its antigen.

In summary, both the galvanostatic and ac impedance measurements support a model for immunosensors in which the observed potentiometric response can be related to modulation of exchange currents resulting from the selective immunoreaction between specific antibody and antigenic ionophore or antigen conjugated with ionophore. Consequently, very simple immunosensors can be constructed for those cases where the antigen has some ionophoric function.

Acknowledgment. We gratefully acknowledge the support of National Institutes of Health Grant GM-25308.

High-Energy Resolution X-ray Photoelectron Spectroscopy Studies of Tetracyanoquinodimethane Charge-Transfer Complexes with Copper, Nickel, and Lithium

John M. Lindquist[†] and John C. Hemminger*

Institute for Surface and Interface Science and Department of Chemistry, University of California, Irvine, California 92717

Received July 28, 1988

X-ray photoelectron spectra are presented for LiTCNQ, Ni(TCNQ)₂·3H₂O, CuTCNQ, and Cu(TCNQ)₂ (TCNQ = tetracyanoquinodimethane). The Cu(TCNQ)₂ compound is shown to be of a mixed valence character: Cu⁺(TCNQ⁻)(TCNQ⁰). The TCNQ component in all the other complexes is well described as TCNQ⁻. The detailed shape of the shakeup intensity observed in both C 1s and N 1s spectra is discussed in comparison with the trend of electrical conductivity in these compounds. We suggest that the valence orbital involved in the strong XPS shakeup intensity for TCNQ⁰ is involved in the conductivity in the charge-transfer complexes.

Introduction

For more than 2 decades the strong electron-acceptor tetracyanoquinodimethane (TCNQ) has been the subject of many studies. Throughout this period a number of intriguing applications have been proposed that make use of this unique molecule and also the charge-transfer complexes it forms with many organic and metal electron-donor species.^{1,2} These applications include use of the charge-transfer complexes in optical recording disks,¹ molecular electronic devices,¹ and corrosion inhibition.²

These applications as well as a fundamental concern with the charge-transfer process have resulted in much interest in the mechanism of TCNQ compound formation.

With regard to charge transfer we are interested in the nature of the TCNQ molecular orbitals involved in this process and how their character changes as a function of charge shifting upon complex formation. Lin et al.³ have

[†] Present address: Aerojet ElectroSystems Co., MS 170-8244, PO Box 296, Azusa, CA 91702.

(1) Potember, R. S.; Hoffman, R. C.; Hu, H. S.; Cocchiaro, J. E.; Viands, C. A.; Poehler, T. O. *Polym. J.* 1987, 19, 147.

(2) Lindquist, J. M.; Giergiel, J.; Hemminger, J. C., data to be published from our laboratory indicates that stable high-temperature TCNQ films can be produced on transition-metal surfaces.

(3) Lin, S. F.; Spicer, W. E.; Schechtman, B. H. *Phys. Rev. B* 1975, 12, 4184.